

Network pharmacology-based identification of the key mechanism of quercetin acting on hemochromatosis

Authors: Haoxuan Ding¹, Lingjun Chen¹, Zuopeng Hong², Xiaonan Yu¹, Zhonghang Wang¹, Jie Feng^{1*}

Affiliations:

1 College of Animal Sciences, Zhejiang University, Key Laboratory of Animal Feed and Nutrition of Zhejiang Province, Hangzhou, 310058, China

2 Research Center of Zhejiang Weifeng Biotechnology Co., Ltd, Hangzhou, 310000, China

*Correspondence to: fengj@zju.edu.cn

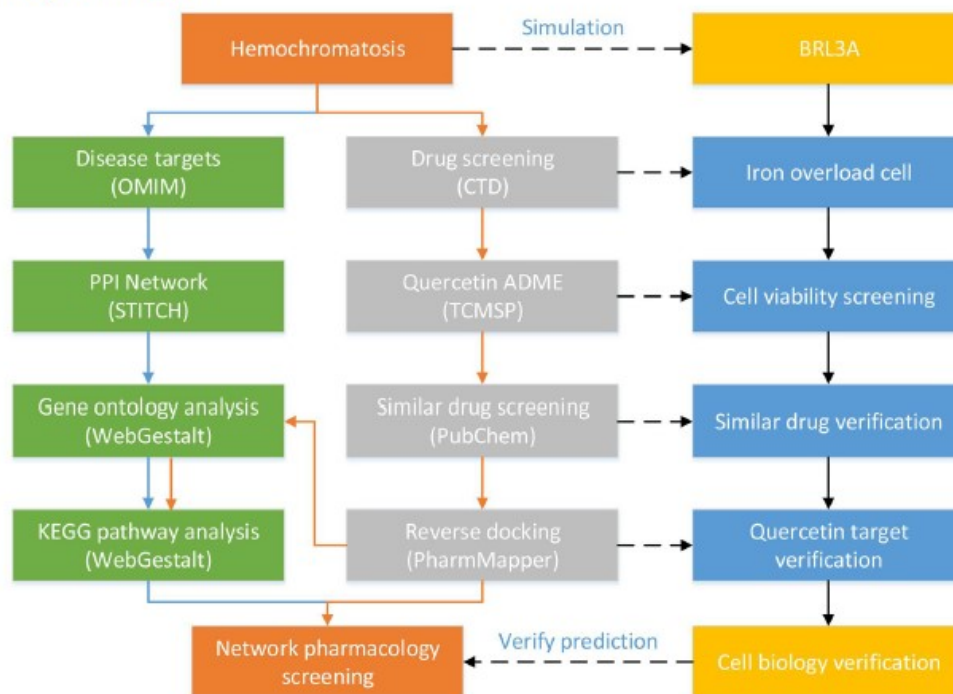
ORCID iD: <https://orcid.org/0000-0002-2690-429X>

Abstract: Hemochromatosis is an iron overload disease, which lacks nutritional intervention strategies. This study explored the protective effect of quercetin on hemochromatosis and its possible mechanism through network pharmacology. We used Online Mendelian Inheritance in Man (OMIM) to screen the disease targets of hemochromatosis, and further constructed a potential protein interaction network through STITCH. The above-mentioned targets revealed by Gene enrichment analysis have played an significant role in ferroptosis, mineral absorption, basal cell carcinoma and related signal pathways. Besides, the drug likeness (DL) of quercetin obtained by Comparative Toxicogenomics Database (CTD) was evaluated by Traditional Chinese Medicine Systems Pharmacology (TCMSP), and potential drug targets identified by PharmMapper and similar compounds identified by PubChem were selected for further research. Moreover, gene

Ontology (GO) and Kyoto Encyclopedia of Genes and Genomes (KEGG) pathway analysis revealed the relationship between quercetin and glycosylation. Furthermore, we performed experiments to verify that the protective effect of quercetin on iron overload cells is to inhibit the production of reactive oxygen species (ROS), limit intracellular iron and degrade glycosaminoglycans. Finally, iron-induced intracellular iron overload caused ferroptosis, and quercetin and fisetin were potential ferroptosis inhibitors. In conclusion, our study revealed the correlation between hemochromatosis and ferroptosis, provided the relationship between the target of quercetin and glycosylation, and verified that quercetin and its similar compounds interfere with iron overload related disease. Our research may provide novel insights for quercetin and its structurally similar compounds as a potential nutritional supplement for iron overload related diseases.

ORIGINAL UNEDITED MANUSCRIPT

Graphical Abstract



Network pharmacology reveals the mechanism of hemochromatosis and predicts the function of natural products.

Keywords: Hemochromatosis; Network pharmacology; Quercetin; Natural products; Ferroptosis;

Glycosylation

ORIGINAL UNEDITED

1. Introduction

Hemochromatosis is a disease caused by excessive iron accumulation in the body due to a high-iron diet, massive blood transfusions, or genetic mutations.¹ Most of hereditary hemochromatosis (HH) is caused by mutations of iron transport related proteins [such as hemochromatosis protein (HFE), blood juvenile (HJV), transferrin receptor 2 etc].² Unlike HH, secondary hemoglobinosis is usually caused by chronic excessive intake of iron.^{1,3} In Hemochromatosis, excessive iron generates reactive oxygen species (ROS) through the Fenton reaction to cause oxidative damage, which ultimately leads to chronic complications such as severe liver cirrhosis, heart disease, and diabetes.^{1,4} At present, the main method of clinical treatment of hemochromatosis is phlebotomy (or bloodletting).^{5,6} With the decrease of iron levels, physical discomfort has been significantly improved, but there is no significant improvement in diseases such as joint disease.⁷ Currently there are relatively few treatment options for HH patients. Therefore, there is an urgent need for a HH adjuvant treatment method that can not only reduce the damage caused by iron deposition in the body, but also alleviate the oxidative stress caused by ROS.

Traditional Chinese medicine (TCM) and natural products are the best sources of active ingredients for drug discovery, and active compounds are beneficial to the treatment of diseases even as nutritional supplements⁸⁻¹⁰. For example, quercetin is a polyphenol widely occurred in fruits and vegetables, and has biological functions such as anti-inflammatory and antioxidant.¹¹ Due to the complexity of TCM, the mechanism of action of the active ingredients in many traditional medicines is still unclear.¹² Network pharmacology, which uses computational methods

to relocate targets, is becoming a new trend in drug screening because of its efficiency, convenience, and targeting.¹³ This field combines computational biology to build a network for exploring drug mechanisms, and systematically observes the effect of the drug on the disease based on drug-gene-disease interaction networks.^{14,15}

In this study, we used the OMIM server to find disease targets for hemochromatosis. Then, we constructed the protein-protein interaction (PPI) network diagram of the disease, and further studied the most critical pathways based on GO and KEGG pathway analysis. Next, we used the CTD database to screen the bioactive compounds related to the treatment of hemochromatosis, and used the TCMSP server to evaluate the drug feasibility of quercetin, and provided more drugs similar to quercetin according to PubChem. Then, the potential targets of quercetin were predicted by calculating the reverse docking, and based on the GO and KEGG pathway analysis selection to analyze the intervention mechanism of quercetin on hemochromatosis. In addition, we also conducted experiments to verify the mechanism of quercetin-mediated treatment of hemochromatosis.

2. Materials and Methods

2.1 Hemochromatosis target identification and PPI network construction

Hemochromatosis targets were obtained from the Online Mendelian Inheritance in Man (OMIM; <https://omim.org/>). OMIM was the authoritative compendium of human genes and genetic phenotypes created by Victor A. McKusick of Johns Hopkins University. The key genes studied for their interaction with hemochromatosis were determined using STITCH server.¹⁶ Briefly, according to the key genes of hemochromatosis obtained from the OMIM database, the correlation between the PPI networks was mapped to understand the coordination between

network components.

2.2 GO and pathway analysis of targets

WebGestalt is a popular tool for gene enrichment analysis.¹⁷ The hemochromatosis gene was imported into the WebGestalt database (<http://www.webgestalt.org/>) for GO and KEGG pathway to further obtain the functional annotation of the target. Following the online instructions, the GO and KEGG path information of hemochromatosis was generated and collected. Moreover, the plant active compound quercetin obtained by subsequent screening was also analyzed by GO and KEGG pathway.

2.3 Acquisition of hemochromatosis related drugs

In order to obtain relevant therapeutic drugs for hemochromatosis, screening was carried out through the comparative toxicological genomics database (CTD, <http://ctdbase.org/>).¹⁸ We selected drugs with hemochromatosis inferred score > 20.0 in the CTD database. A high inference score means a strong correlation between the target and the active compound.¹⁹ In addition, we selected the first-ranked plant flavonoids from the selected potential drugs for subsequent analysis and verification.

2.4 Evaluation of drug-likeness using the TCMSP Server

TCMSP (<https://tcmsp.w.com/tcmssp.php>) is a platform that captures the relationship between drugs, targets and diseases.²⁰ In the platform, the ADME-related properties of natural compounds would be calculated and analyzed.²¹ The specific calculation process is described in detail in the reference.⁸ According to the CTD results, the chemical name quercetin was used as the search term to analyze its drug properties at the molecular level.

2.5 Similar drug screening and computational target fishing

In order to expand the bioactive components that may potentially treat hemochromatosis, we sorted out the top 30 compounds with similar structures of quercetin (CID: 5280343) through the PubChem database. An sdf file for quercetin was downloaded from the PubChem database and upload it to the pharmapper server. PharmMapper is a reverse docking server that identifies potential protein targets of small molecule compounds through pharmacophore mapping methods.²² Quercetin reverse docking obtained 300 targets sorted in descending order according to the normalized fit score, and then we selected the targets with a normalized fit score > 0.6 for GO and KEGG analysis.

2.6 Establishment of the iron overload model of BRL3A cells

Rat liver cells BRL3A were obtained from American Type Culture Collection (ATCC, Manassas, VA, USA). BRL3A cells were cultured in Dulbecco's modified Eagle's medium (DMEM) supplemented with 10% fetal bovine serum and 1% penicillin-streptomycin in a humidified incubator with 5% CO₂ at 37°C. Reagents and culture flasks were purchased from Gibco (Gibco, Life Technologies, CA, USA).

In order to simulate the iron overload caused by hemochromatosis, we used a highly lipophilic Fe8HQ to rapidly increase the intracellular iron content. The preparation method of Fe8HQ is that ferric chloride and 8-hydroxyquinoline are dissolved in dimethyl sulfoxide (DMSO) at a molar ratio of 1: 2, and then filtered through a 0.22 μm filter membrane. The relevant reagents for configuring Fe8HQ were purchased from Sigma-Aldrich. The iron source used has previously been reported in the literature.²³ Then we determined iron indicator to judge the status of our iron overload model. The iron fluorescence staining was as previously reported in the literature,²⁴ with

minor modifications. BRL3A cells were seeded at a density of 1×10^4 cells/well in 96 well plates. One day later, the medium was discarded, and the cells were rinsed twice with PBS before being treated with DMEM containing different concentrations (0, 2.5, 5, 10, 20 μ M) of iron for 3h. Moreover, after the same washing procedure, BRL3A cells were incubated with 5 μ M iron for 0, 0.5, 1, 2, 3 h. After treating with iron for indicated time, cells were washed with PBS twice and stained with 10 μ M Phen Green SK (Thermo Fisher P14313) in PBS for 5 min in culture incubator. The stained cells were washed twice with PBS, and iron indicator was measured with a fluorescence microplate reader ($\lambda = 490/520$ nm, SpectraMax M5, Molecular Devices, Sunnyvale, CA, USA). To detect the effect of the compound on the iron indicator of BRL3A cells, the cells were treated with different concentrations of quercetin or fisetin (0, 2, 4, and 8 μ M) under the background of exogenous iron (5 μ M). The effects of quercetin (Que) and fisetin (Fis) treatments on iron indicator were determined by similar methods.

2.7 Cell viability and morphology

The effect of iron on the viability of BRL3A cells were measured by the CCK-8 assay (MedChem Express, Princeton, NJ, USA) as formerly described.^{23,24} The seeded cells were treated with various concentrations of iron (0, 0.5, 1, 2.5, 5, 10, 20, 40, 60 μ M) for 3 h. To detect the effects of quercetin or fisetin on the viability of iron overload cells, BRL3A cells were treated with 5 μ M iron for 3 h followed by treatment with different concentrations of quercetin or fisetin (0, 2, 4 and 8 μ M) respectively. Then the cell viability was assessed by CCK8. To visualize the cell morphology, the characteristic cell morphology was observed with microscope. The LEICA DCF295 microscope used phase contrast images of static bright field cells equipped with 20 \times phase contrast objectives.²³

To determine that quercetin/fisetin relieves cell death after iron overload, cells were pretreated with 5 μM iron for 0.5 h, washed with PBS, and then treated with different concentrations of quercetin or fisetin (0, 2, 4 and 8 μM) for another 2.5h. After the incubation, the cell viability was performed in accordance with the above-mentioned CCK8 manufacturer's instruction.

To detect the effect of ferroptosis inhibitors on the viability of iron overload cells, cells were seeded in 96-well plates at a density of 1×10^4 /well and treated with 5 μM iron, 5 μM iron + 10 μM liproxstatin-1 (Lip-1), 5 μM iron + 10 μM ferrostatin-1 (Fer-1), 10 μM Lip-1, 10 μM Fer-1 for 6 or 12 h. After the incubation, the cell viability was performed in accordance with the above-mentioned CCK8 manufacturer's instruction.

To detect the effect of polyphenols (quercetin or fisetin) on ferroptosis, cells were seeded in 96-well plates at a density of 1×10^4 /well and treated with 2 μM RSL3 (ferroptosis inducer), 2 μM RSL3 + 8 μM Que/Fis, 2 μM RSL3 + 10 μM Fer-1, 8 μM Que/Fis, 10 μM Fer-1 for 3 h. After the incubation, the cell viability was performed in accordance with the above-mentioned CCK8 manufacturer's instruction. To visualize the cell morphology, the characteristic cell morphology was observed with microscope.

2.8 Assessment of reactive oxygen species production

To detect the effect of the compound on the reactive oxygen species (ROS) production of BRL3A cells, the seeded cells were treated with 5 μM iron for 3 hours, with different concentrations of quercetin or fisetin (0, 2, 4, and 8 μM). Then the cells were washed with PBS twice and stained with 5 μM CM-H2DCFDA (C6827, Invitrogen) in PBS for 5 min in culture incubator. The stained cells were washed twice with PBS, and measured with a fluorescence

microplate reader ($\lambda = 493/520$ nm).

To determine that quercetin/fisetin relieves the increase of intracellular ROS after iron overload, cells were pretreated with 5 μ M iron for 0.5 h, washed with PBS, and then treated with different concentrations of quercetin or fisetin (0, 2, 4 and 8 μ M) for another 2.5h. After the incubation, the intracellular ROS was performed in accordance with the above-mentioned ROS manufacturer's instruction.

2.9 Toluidine blue staining and sulfated glycosaminoglycan quantification

To detect the effect of quercetin on glycosaminoglycan (GAG) synthesis in iron-overloaded BRL3A cells, the cells were seeded in a 6-well plate and treated with 5 μ M iron for 3 h followed by treatment with quercetin (0 or 8 μ M). The cells were washed twice with PBS and fixed in 4% paraformaldehyde for 5 minutes. Then, the cells were stained with toluidine blue solution for 10 minutes in the dark. Finally, the cells were washed with PBS and observed with the LEICA DCF295 microscope.

To measure the content of GAG in cells, a GAG ELISA kit was used as formerly described.²⁵ Briefly, the cells were seeded in a 6-well plate and treated with 5 μ M iron for 3 h followed by treatment with quercetin (0 or 2, 4, 8 μ M). After the sample was collected by trypsin digestion, the assay was performed according to the GAG ELISA instructions. Finally, a microplate reader was used to measure the colored reaction products at 450 nm.

2.10 Annexin V/PI binding assay

In order to determine the type of cell death of BRL3A cells caused by Fe8HQ, The FITC-Annexin V/PI technique was performed for quantitation of apoptotic/necrotic cell death.

Cell lines were seeded into 6-well plates and treated with 5 μ M iron, 2 μ M RSL3, 2 μ M RSL3+8

μM Que, 2 μM RSL3+ 10 μM Fer-1, 8 μM Que, 10 μM Fer-1 for 3 hour. At the end of the treatment time, the cells were washed twice by PBS and detached by accutase. Afterward, the cells were resuspended in 500 μL binding buffer and 5 μL of FITC-conjugated Annexin V was added to cell suspensions. Hereafter, 5 μL of PI (propidium iodide) staining solution was added to the cells and incubated at room temperature under dark condition for 15 min. The FITC-labeled Annexin V-positive cells were measured in the FL1 channel ($\lambda = 488/510$ nm) and the PI-labeled cells were measured in the FL2 channel ($\lambda = 581/591$ nm) using FACS Calibur flowcytometry.

2.11 Lipid ROS assay using flow cytometer

Lipid ROS levels were determined using BODIPY 581/591 C11 dye as previously reported.²³ Briefly, cell lines were seeded into 6-well plates and treated with 5 μM iron, 5 μM iron + 8 μM Que, 5 μM iron + 10 μM Lip-1, 2 μM RSL3, 2 μM RSL3 + 8 μM Que, 2 μM RSL3 + 10 μM Fer-1 for 3 hour. At the end of time, culture media was replaced with 1 ml media containing 5 μM of BODIPY 581/591 C11 dye for 30 min. Cells were harvested and washed twice with Hank's Balanced Salt Solution (HBSS) followed by resuspending in 500 μL of HBSS. Afterward, lipid peroxidation was analyzed with a flow cytometer, and the ratio of the intensity of the FL1 channel to the intensity of the FL2 channel was calculated.

2.12 Statistical analyses

All data were presented as the means or \pm SD. Statistical analyses were performed by using one-way ANOVA with post hoc Bonferroni test on GraphPad Prism (version 5.01) software. The changes between the two groups were analyzed using Student's t-test. *P* values < 0.05 were considered to be statistically significant.

3 Results

3.1 Hemochromatosis target identification and PPI network construction

In order to determine the disease target, we collected the target genes of hemochromatosis from the OMIM database. As shown in Table 1, we had discovered 7 key target genes for hemochromatosis. Moreover, we used STITCH to obtain the PPIs among 7 simulated targets and the clear target, as shown in Figure 1. The large nodes represented proteins and the edges indicated their relations. Due to the limitations of the current research, some protein interactions were still unclear, but the network constructed by this research provided an intuitive link to genes related to hemochromatosis.

3.2 GO and KEGG analysis of targets

To further investigate the interaction network, we performed analyses using WebGestalt database. Gene Ontology Biological Process (GOBP) analysis was performed to verify the targets of hemochromatosis. Figure 2 revealed the first 10 enriched GOBP entries. We could infer that many targets were closely related to hemochromatosis, such as cellular iron ion homeostasis, iron ion homeostasis, cellular transition metal ion homeostasis, transition metal ion homeostasis, iron ion transport. GOBP analysis also clearly pointed out that the key to hemochromatosis is to regulate iron homeostasis, which provided a reference for understanding the biological process of hemochromatosis. Moreover, Gene Ontology Cellular Component (GOCC) analysis was performed to verify the targets of hemochromatosis. Figure 2 revealed the first 10 enriched GOCC entries, we could realize that HFE-transferrin receptor complex, plasma membrane receptor complex, receptor complex, plasma membrane protein complex, integral component of plasma membrane are related to hemochromatosis. In addition, Gene Ontology Molecular Function

(GOMF) Analysis also contributed to our understanding of hemochromatosis (Figure 2). GOMF analysis showed that co-receptor binding, transferrin receptor binding, iron ion transmembrane transporter activity, transition metal ion transmembrane transporter activity, and signaling receptor binding had important molecular functions in hemochromatosis. To identify signaling pathways involved in hemochromatosis, We mapped the KEGG database and found that 4 KEGG pathways were significantly enriched. The top 8 enriched pathways were shown in Figure 3, hemochromatosis-related genes were highly clustered in several signaling pathways, such as “Ferroptosis”, “Mineral absorption”, “Basal cell carcinoma” and “TGF-beta signaling pathway”, suggesting that ferroptosis may have an important function in hemochromatosis.

3.3 ADME-Related Properties of quercetin and screening of similar drugs

Potential drugs related to hemochromatosis came from the CTD, As shown in Table 2, a total of 17 hemochromatosis-related drugs were screened with an inference score > 20. From the perspective of nutritional supplements, we selected the first-ranked plant flavonoids quercetin from the selected potential drugs for subsequent analysis and verification. TCMSP provides information on important ADME-related properties such as human oral bioavailability (OB), drug-likeness (DL), and Lipinski's rule of five (MW, AlogP, TPSA, Hdon, Hacc). ADME-related properties of quercetin were investigated in depth by TCMSP (Table 3). Notably, the DL of quercetin was calculated to be 0.28, and $DL > 0.18$ was generally considered to have the potential to become a drug. In order to expand the bioactive components that may potentially treat hemochromatosis, we sorted out the top 30 compounds with similar structures of quercetin (CID: 5280343) through the PubChem database (Table 4).

3.4 Identification of potential targets and enrichment analysis

Pharmapper was used to predict the potential targets of quercetin. Table 5 showed the potential protein targets with a normalized fit score greater than 0.6 using the obtained pharmacophore model. The 13 possible interaction proteins were further studied and analyzed by GO and KEGG pathway. As shown in Figure 4, the top five biological processes were protein glycosylation in Golgi, fucose catabolic process, L-fucose metabolic process, L-fucose catabolic process, cytoskeletal anchoring at plasma membrane, which reflected the correlation between quercetin and glycosylation. Moreover, cellular component and molecular function also confirmed the correlation between quercetin and glycosylation. In addition, Quercetin-related targets were involved in 8 KEGG pathways, especially Glycosaminoglycan biosynthesis, N-Glycan biosynthesis, Salmonella infection, and Transcriptional misregulation in cancer were significantly upregulated (Figure 5).

3.5 Establishment of iron overload cell model

The Phen Green-SK stained BRL3A cells were used to observe the iron indicator with a microplate reader. Iron treatment leads to the quenching of Phen Green SK in the cells, which indicates an increase in iron. To further quantify the increase in intracellular iron, after treatment with iron at different concentrations, the labile iron levels of BRL3A cells were recorded, as shown in Figure 6 A. The fluorescence of intracellular iron indicator showed a dose-dependent quenching, and the fluorescence of 2.5 μM iron treatment for 3 hours was significantly lower than that of the control group. Moreover, as shown in Figure 6 B, the fluorescence of 5 μM iron treatment for 0.5 hours was significantly lower than that of the control group, which means that it only takes half an hour for iron to enter BRL3A cells. As shown in Figure 6 C and D, iron

concentrations of 0-1 μ M had no cytotoxic effect on the viability of BRL3A cells. Compared with the control group, 5 μ M iron treatment significantly reduced cell viability ($P < 0.05$). The half-maximal inhibitory concentration (IC₅₀) of iron in BRL3A cells was less than 5 μ M. Thus, iron at the concentrations of 5 μ M was chosen for further study. In addition, the cell morphology obviously showed swelling under high-dose iron treatment (20 μ M iron), suggesting that the results of cell viability and cell morphology are consistent. In a word, these results indicated that we had established a model of iron overload in BRL3A cells.

3.6 Quercetin protection BRL3A from iron-induced cell death

In order to verify the reliability of quercetin obtained from network pharmacology in intervention of hemochromatosis, we used quercetin for intervention in the iron overload cell model. The viability of BRL3A cells decreased after iron treatment (5 μ M), otherwise, quercetin could reverse this effect in a dose-dependent manner, which indicated that quercetin could promote the proliferation of iron overload cells (Figure 7 A). In addition, structure determines function, which is true not only for proteins, but also for flavonoids. Therefore, we also selected fisetin obtained in PubChem database to rescue iron overload cells. Consistent with expectations, fisetin also showed the same rescuing effect on iron overload cells as quercetin (Figure 7 B). Because the cell morphology did not change significantly within a short period of time (3h) after 5 μ M iron treatment, we prolonged the treatment time to obtain a more intuitive comparison of cell morphology. As shown in Figure 7 C, the intervention of quercetin or fisetin could protect BRL3A cells from iron overload damage. In order to check whether the rescue of quercetin on cell death is only due to its iron chelation potential, when cells were pre-cultured with iron, quercetin still showed an interventional effect on iron overloaded cells (Figure 7 D). Consistent with the results

of quercetin, fisetin also showed a relief effect on iron-pretreated cells (Figure 7 E). In short, quercetin protected BRL3A cells from iron-induced cell death.

3.7 Quercetin-mediated iron, ROS, and GAG clearance

The accumulation of iron in cells generates ROS through Fenton reaction, which is one of the important reasons why iron induces cell death. To test whether quercetin contributes to eliminating iron and ROS in cells, we performed corresponding fluorescent staining and measured it with a microplate reader. After BRL3A cells were treated with 5 μ M iron, the increase of intracellular iron caused fluorescence quenching (Figure 8 A). Quercetin intervention helped restore intracellular iron indicator fluorescence, especially 8 μ M, which meant that quercetin could limit intracellular iron (Figure 8 A). Similarly, fisetin also showed the elimination of intracellular iron indicator like quercetin (Figure 8 B). After intracellular iron overload, the ROS increased rapidly, and the intervention of quercetin significantly reduced intracellular ROS (Figure 8 C). Consistent with expectations, fisetin also reduced the intracellular ROS after iron overload (Figure 8 D). To further examine the ROS scavenging effect of quercetin on iron-pretreated cells, we measured the level of intracellular ROS. Interestingly, quercetin showed a better ROS scavenging effect on iron-pretreated cells than iron co-culture treatment (Figure 8 E). Moreover, different concentrations of fisetin also showed an effective ROS scavenging effect on iron-pretreated cells (Figure 8 F). Pharmapper predicted that the potential target of quercetin reflects the correlation between quercetin and glycosylation, and we further verified it at the cellular level. Toluidine blue staining showed a significant increase in the synthesis of glycosaminoglycans in the Fe group, but quercetin significantly reversed the increase of glycosaminoglycan (Figure 8 G). Moreover, the GAG assay also indicated that quercetin significantly inhibited iron-induced GAG increase

(Figure 8 G). Collectively, these results indicated that quercetin could effectively reverse iron-induced cell death by limiting intracellular iron, ROS and GAG.

3.8 Iron-induced intracellular iron overload causes ferroptosis

In order to detect the mode of cell death caused by iron overload in BRL3A cells, we used FITC-Annexin V/PI technique to quantify apoptotic/necrotic cell death and detect phosphatidylserine externalization. Annexin V/PI staining confirmed that iron overload significantly induced cell late apoptosis and necrosis, and a large number of cells with damaged membranes appeared (Figure 9 A). Furthermore, classic ferroptosis inhibitors (lipoxstatin-1, ferrostatin-1) were used to interfere with iron-induced cell death. As shown in Figure 9 B and C, lipoxstatin-1 and ferrostatin-1 significantly increased the cell viability of iron overloaded cells. As lipid peroxidation is a character of ferroptosis, we next determined the lipid ROS level. Consistently, treatment of BRL3A cells with iron resulted in a significant increase in lipid ROS, while incubation with Que or Lip-1 significantly reduced the increase in lipid ROS (Figure 9 D). These results suggested iron-induced intracellular iron overload causes ferroptosis.

3.9 Identification of quercetin as a potent ferroptosis inhibitor

Ferroptosis is a regulated form of cell death driven by loss of activity of the lipid repair enzyme glutathione peroxidase 4 (GPX4) and subsequent accumulation of lipid-based ROS. RSL3 is a classic ferroptosis inducer, which induces cell ferroptosis by inhibiting GPX4. As shown in Figure 10A, we treated BRL3A cells with RSL3 to induce ferroptosis. Interestingly, quercetin abolished cell death induced by RSL3 in BRL3A cells (Figure 10 A), just as Fer-1 did, which is a selective inhibitor of ferroptosis. Consistently, fisetin also showed the same inhibition of ferroptosis as quercetin (Figure 10 B), which may suggest that we provide a series of polyphenols

(table 4) as ferroptosis inhibitors. Moreover, treatment of BRL3A cells with RSL3 resulted in a significant increase in lipid ROS, while incubation with Que or Fer-1 terminated the increase of lipid ROS (Figure 10 C). As ferroptosis coincided with morphologic changes, microscopy studies revealed that Que or Fer-1 could protect RSL3-induced outer membrane rupture in BRL3A cells (Figure 10 D). Consistently, Annexin V/PI staining also confirmed the intervention of quercetin on the ferroptosis of BRL3A cells (Figure 10 E). Together, these data supported the hypothesis that quercetin is a promising nutritional intervention to treat iron overload disease by inhibiting ferroptosis in liver cells.

4 Discussion

Hemochromatosis is characterized by improper high iron absorption that leads to excessive iron deposition in the organs, and lack of nutritional measures to relieve the symptoms of hemochromatosis.²⁶ Most HH cases are attributed to mutations in the HFE gene, which limits the HFE-TFR2-HJV complex to trigger the BMP/SMAD signaling pathway to hepcidin expression.²⁷ We constructed a PPI network to show the correlation of 7 key target genes for hemochromatosis. Moreover, we also provided interaction proteins that depended on 7 key genes of hemochromatosis. These interactions may have guiding significance in the treatment of HH patients.

In our study, GOBP analysis clearly pointed out that the key to hemochromatosis is to regulate iron homeostasis. Genes related to hemochromatosis such as transferrin receptor-2 (TfR2), hemoglobin (HJV) or hepcidin (HAMP) are closely related to iron metabolism, and gene mutations could easily cause inappropriate low hepcidin expression and lead to organ iron overload.²⁸ Vitamin A deficiency is positively correlated with the up-regulation of liver HAMP

expression in vivo, without affecting the expression of iron absorption-related genes, which may help to interfere with the low expression of hepcidin in hemochromatosis.^{26,29} Moreover, GOCC analysis revealed the importance of HFE-transferrin receptor complex in hemochromatosis. HFE interacts with TfR2 on the cell membrane, and HFE and BMP type receptor BMPRI1A(ALK3) regulate iron absorption through hepcidin.³⁰ Therefore, the HFE/TfR2 complex acts as an iron sensor in hepatocytes and controls iron homeostasis.³¹ In addition, GOMF analysis showed co-receptor binding has important molecular functions in hemochromatosis. HJV is an inducer of hepcidin expression and acts as a co-receptor for bone morphogenetic protein-6 (BMP-6).³² The expression of hepcidin induced by BMP is inhibited by the membrane-bound serine protease matriptase-2 (MT-2), and MT-2 inhibits the expression of hepcidin by cleaving the BMP co-receptor HJV.³³ In the KEGG enrichment assay, we noticed that the ferroptosis signaling pathway is an important target pathway in hemochromatosis. In recent years, a form of iron-dependent oxidative cell death called ferroptosis has been discovered.³⁴ The ferroptosis signaling pathway has an important influence on iron overload-related diseases, and iron overload plays a key role in triggering Slc7a11-mediated ferroptosis.² Although the current common treatment for hemochromatosis is still phlebotomy,²⁶ ferroptosis related targets provide new possibilities for the treatment of hemochromatosis. In conclusion, targeting the ferroptosis signal pathway may be a potential therapeutic approach for hemochromatosis.

Flavonoids are bioactive secondary metabolites synthesized in plants with strong antioxidant, anti-cancer activity, immune regulation and are widely used in a variety of acute and chronic human diseases.³⁵ Network pharmacology and systems biology could explain the role of flavonoids in biological networks from a macro perspective, and provide new technical means for

the study of the mechanism of plant active compounds.¹⁴ We chose the plant flavonoid quercetin to be widely found in common fruits and vegetables such as onions, apples, and oranges.¹¹ Bioinformatics could simulate the ability of pharmacokinetics, metabolism and toxicity to simplify and accelerate the drug discovery process.³⁶ The performance of quercetin complies with Lipinski's "rule of 5",⁸ which means that quercetin is a potential drug candidate. Moreover, the DL of quercetin was calculated to be 0.28, and $DL > 0.18$ is the standard for screening biologically active compounds based on system pharmacology.²¹ According to the adaptation of structure and function, we also screened out 30 compounds that are similar in structure to quercetin. On the one hand, the B ring of quercetin has a catechol moiety and multiple free hydroxyl structures, which drive its outstanding iron chelating properties.^{11,37} On the other hand, some studies have shown that the 3-hydroxy-4-keto (C ring) is the main site for iron binding.^{38,39} Taken together, the plant polyphenol quercetin and its structurally similar compounds may be a nutrient that interferes with hemochromatosis.

Target identification is the key to elucidating the mechanism of flavonoids, and various silico target fishing methods are widely used.⁴⁰ We screened 13 putative quercetin targets using computational tools and further analyzed them through GO and KEGG pathways. GO and KEGG analysis showed that there is a strong correlation between quercetin and glycosylation, and we also carried out experimental verification in the follow-up. Glycosylation of flavonoids is to couple flavonoid aglycones and glycosyl groups in a conjugated form, which would increase water solubility and specific targeting, and reduce toxic and side effects.⁴¹ In vivo experiments previously reported that quercetin could protect vascular dysfunction in patients with metabolic syndrome by interfering with the formation of advanced glycation end products (AGEs).⁴²

Moreover, *in vitro* experiments showed that the glycosylated derivative quercetin 3-O-xyloside has anti-pancreatitis activity by reducing the production of intracellular ROS and ER stress response and enhancing the death of apoptotic cells.⁴³ In short, we may need to focus on the role of quercetin and glycosylation in acute and chronic diseases.

Iron is an essential trace element, and the balance of iron in the body is the basis for various life activities.^{44,45} Iron overload causes ROS generation, lipid peroxidation and DNA base modification, which threatens the body's metabolism.^{46,47} Liver transplantation normalized hepcidin secretion and prevented liver iron overload, which confirmed that the key to intervention in HFE-related hemochromatosis is liver health.⁴ Therefore, we selected rat liver cells (BRL3A) close to clinical application for *in vitro* experiments. In our study, we established a model of iron overload in BRL3A cells and determined the dose for subsequent evaluation. Then, we described that the protective effect of quercetin on iron overloaded cells was mediated by limiting intracellular iron, inhibiting ROS production and degrading glycosaminoglycans, thereby alleviating iron-induced cell death. It was previously reported that quercetin effectively reduces iron deposition and reduces lipid peroxidation and protein oxidation in the liver of iron-overloaded mice,^{48,49} and we had also verified this *in vitro* experiments. Moreover, alcoholic liver disease (ALD) causes liver labile iron pool and lysosomal iron retention due to iron overload, and quercetin can reverse these effects.⁵⁰ It should be noted that the Phen Green SK probe in this study is not specific for Fe²⁺ or Fe³⁺, and it also interacts with other metal ions to produce interference signals, which may affect the quantification of intracellular iron levels. Novel high-specificity Fe²⁺ probes such as iron probe 1 (IP-1) or Ferro-RhoNox are more suitable for quantifying intracellular iron levels. The catechol and 3-hydroxy-4-keto structure of quercetin drives its excellent iron

chelating properties.^{11,37-39} In this study, whether it was iron pretreatment or iron co-incubation, quercetin could play a function of scavenging intracellular ROS to avoid cell death, which means that quercetin may limit the production of ROS by chelating extracellular or intracellular iron. Besides, quercetin up-regulates the expression of transforming growth factor β (TGF- β) and insulin-like growth factor (IGF), promotes the synthesis of glycosaminoglycans in chondrocytes, and shows the potential for treating osteoarthritis.²⁵ Quercetin has the potential to be used as a nutritional supplement for the regulatory function of iron overload-related diseases, which helps to cure chronic diseases. In addition, the polyphenol fisetin, which has a similar structure to quercetin, not only acts as an iron chelator and inhibits oxidative stress, but also exhibits anti-amyloidogenesis and fibril destabilization activities.⁵¹ In a word, the protective effect of quercetin on iron-overloaded cells is to limit intracellular iron, inhibit the production of ROS and degrade glycosaminoglycans, which may help nutritional supplement strategies for many chronic diseases.

In recent years, the relationship between iron overload and ferroptosis has received widespread attention. Previous study reported that iron overload potently induces ferroptosis in murine primary hepatocytes.² Our previous study also showed that iron overload could cause ferroptosis in HT-1080 cells.²³ The results of this study are consistent with those of previous studies, indicating that iron induced intracellular iron overload contributes to the occurrence of ferroptosis. Moreover, iron overload may not only lead to ferroptosis, but also cause apoptosis, necrosis and other cell death. The causes of multiple cell deaths due to iron overload may be the cell type, iron source, dosage and other factors. It has been reported that ferroptosis firstly occurred in a relatively low concentration of iron overload group, and then apoptosis appeared in

response to the increased iron doses.⁵² Interestingly, we found that quercetin, a polyphenol, significantly inhibited RSL3 induced-ferroptosis, increased the cell viability and decreased cellular lipid ROS. Ferroptosis was blocked by quercetin, consistent with previous studies on kidney and bone marrow mesenchymal stem cells^{53,54}. Previous study has emphasized the importance of liver ferroptosis in hemochromatosis,² and we found that quercetin could inhibit ferroptosis of liver cells. However, quercetin has poor bioavailability and solubility, which may limit its application^{53,55}. Moreover, we provided a series of polyphenols with similar structure to quercetin, and confirmed that fisetin could also alleviate ferroptosis, which provides clues for us to find inhibitors of ferroptosis. To date, ferroptosis has been indicated to be the shared pathological process in diverse diseases, such as hemochromatosis, acute kidney injury and neurodegenerative diseases.^{2,11} Quercetin is not only an inhibitor of ferroptosis, it also has intervention effect on iron overload related diseases. Within the field of human iron biology, great progress has been made in the interaction between quercetin and iron. Based on density functional methods, quercetin is found to stably chelate Fe²⁺ in the form of either a neutral or a deprotonated isoform.⁵⁶ Besides, quercetin helps to repair the destruction of GPX4 caused by ferroptosis and eliminate lipid ROS.⁵³ Moreover, Quercetin participates in the expression of iron metabolism-related genes (such as ferroportin and hepcidin) to regulate iron absorption.^{57,58} Furthermore, quercetin alleviates oxidative damage by activating nuclear factor erythroid 2-related factor 2 (Nrf2) signaling.^{59,60} All in all, iron-induced intracellular iron overload caused ferroptosis, and quercetin and fisetin were potential ferroptosis inhibitors.

5. Conclusion

In this study, we used OMIM to screen the disease targets of hemochromatosis, and further constructed a potential protein interaction network through STITCH. Moreover, GO and KEGG pathway analysis clarified the association between hemochromatosis-related genes and iron overload. Besides, the DL of quercetin obtained by CTD was evaluated by TCMSP, and potential drug targets identified by PharmMapper and similar compounds identified by PubChem were selected for further research. In addition, GO and pathway analysis revealed the relationship between quercetin and glycosylation. Furthermore, we performed experiments to verify that the protective effect of quercetin on iron-overloaded cells is to limit intracellular iron, inhibit the production of ROS and degrade glycosaminoglycans. Finally, iron-induced intracellular iron overload caused ferroptosis, and quercetin and fisetin were potential ferroptosis inhibitors. Our research may provide novel insights for quercetin and its structurally similar compounds as a potential nutritional supplement for iron overload related diseases.

Conflicts of Interest

The authors declare no conflict of interest.

Data availability statement

The datasets generated during and/or analysed during the current study are available from the corresponding author on reasonable request.

Acknowledgements

This research was funded by the Natural Science Foundation of China (No.31772607), Zhejiang Provincial Key Research and Development Program (2019C02051) and National Key

Technologies R & D Program (2016YFD0501201). We are grateful for the founders and maintainers of OMIM, STITCH, WebGestalt, CTD, TCMSP, PubChem, PharmMapper. Happy New Year !

References:

1. C. Oh, Y. Moon, Dietary and Sentinel Factors Leading to Hemochromatosis. *Nutrients*, 2019, **11**, 1047, DOI: 10.3390/nu11051047.
2. H. Wang, P. An, E. Xie, Q. Wu, X. Fang, H. Gao, Z. Zhang, Y. Li, X. Wang, J. Zhang, G. Li, L. Yang, W. Liu, J. Min, F. Wang, Characterization of Ferroptosis in Murine Models of Hemochromatosis. *Hepatology*, 2017, **66**, 449-465, DOI: 10.1002/hep.29117.
3. R. Lands, E. Isang, Secondary Hemochromatosis due to Chronic Oral Iron Supplementation. *Case Reports in Hematology*, 2017, **2017**, 2494167. DOI: 10.1155/2017/2494167.
4. L. W. Powell, R. C. Seckington, Y. Deugnier, Haemochromatosis. *Lancet*, 2016, **388**, 706-716, DOI: 10.1016/S0140-6736(15)01315-X.
5. F. Odufalu, K. Harris, Hemochromatosis? When Bloodletting Is Not the Cure A Teachable Moment. *Jama Intern Med.*, 2017, **177**, 15-16, DOI: 10.1001/jamainternmed.2016.5872.
6. R. Deitenbeck, T. Zeiler, Hereditary Hemochromatosis: Patient or Donor? *Transfusionsmedizin*, 2018, **8**, 40-44, DOI: 10.1055/s-0043-121418.
7. J. Alexander, K. V. Kowdley, HFE-associated hereditary hemochromatosis. *Genet Med*, 2009, **11**, 307-313, DOI: 10.1097/GIM.0b013e31819d30f2.
8. S. Chen, M. Cui, Systematic Understanding of the Mechanism of Salvianolic Acid A via Computational Target Fishing. *Molecules*, 2017, **22**, 644, DOI: 10.3390/molecules22040644.
9. B. Shen, A New Golden Age of Natural Products Drug Discovery. *Cell* 2015, **163**, 1297-1300,

DOI: 10.1016/j.cell.2015.11.031.

10. S. Hongwei, L. Dongmin, Dietary antiaging phytochemicals and mechanisms associated with prolonged survival. *J Nutr Biochem.*, 2014, **25**, 581-591, DOI: 10.1016/j.jnutbio.2014.02.001.
11. L. Xiao, G. Luo, Y. Tang, P. Yao, Quercetin and iron metabolism: What we know and what we need to know. *Food Chem Toxicol.*, 2018, **114**, 190-203, DOI: 10.1016/j.fct.2018.02.022.
12. Y. Bi, L. Zhang, S. Chen, Q. Ling, Antitumor Mechanisms of Curcuma Rhizoma Based on Network Pharmacology. *Evid-Based Compl Alt.*, 2018, **2018**, 1-9, DOI: 10.1155/2018/4509892.
13. M. R. Hurle, L. Yang, Q. Xie, D. K. Rajpal, P. Sanseau, P. Agarwal, Computational Drug Repositioning: From Data to Therapeutics. *Clin Pharmacol Ther.*, 2013, **93**, 335-341, DOI: 10.1038/clpt.2013.1.
14. C. Jing, Z. Sun, X. Xie, X. Zhang, S. Wu, K. Guo, H. Bi, Network pharmacology-based identification of the key mechanism of Qinghuo Rougan Formula acting on uveitis. *Biomed Pharmacother.*, 2019, **120**, 109381, DOI: 10.1016/j.biopha.2019.109381.
15. S. Chen, H. Jiang, Y. Cao, Y. Wang, Z. Hu, Z. Zhu, Y. Chai, Drug target identification using network analysis: Taking active components in Sini decoction as an example. *Sci Rep-Uk.*, 2016, **6**, 24245, DOI: 10.1038/srep24245.
16. R. Anupama, S. S. Lulu, A. Mukherjee, S. Babu, Cross-regulatory network in *Pseudomonas aeruginosa* biofilm genes and TiO₂ anatase induced molecular perturbations in key proteins unraveled by a systems biology approach. *Gene* 2018, **647**, 289-296, DOI: 10.1016/j.gene.2018.01.042.

17. Y. Liao, J. Wang, E. J. Jaehnig, Z. Shi, B. Zhang, WebGestalt 2019: gene set analysis toolkit with revamped UIs and APIs. *Nucleic Acids Res.*, 2019, **47**, W199-W205, DOI: 10.1093/nar/gkz401.
18. A. P. Davis, C. J. Grondin, R. J. Johnson, D. Sciaky, R. McMorran, J. Wieggers, T. C. Wieggers, C. J. Mattingly, The Comparative Toxicogenomics Database: update 2019. *Nucleic Acids Res.*, 2019, **47**, D948-D954, DOI: 10.1093/nar/gky868.
19. L. Zhang, M. Cui, S. Chen, Identification of the Molecular Mechanisms of Peimine in the Treatment of Cough Using Computational Target Fishing. *Molecules*, 2020, **25**, 1105, DOI: 10.3390/molecules25051105.
20. J. Ru, P. Li, J. Wang, W. Zhou, B. Li, C. Huang, P. Li, Z. Guo, W. Tao, Y. Yang, X. Xu, Y. Li, Y. Wang, L. Yang, TCMSP: a database of systems pharmacology for drug discovery from herbal medicines. *J Cheminformatics.*, 2014, **6**, 13, DOI: 10.1186/1758-2946-6-13.
21. T. Pei, C. Zheng, C. Huang, X. Chen, Z. Guo, Y. Fu, J. Liu, Y. Wang, Systematic understanding the mechanisms of vitiligo pathogenesis and its treatment by Qubaibabuqi formula. *J Ethnopharmacol.*, 2016, **190**, 272-287, DOI: 10.1016/j.jep.2016.06.001.
22. X. Wang, Y. Shen, S. Wang, S. Li, W. Zhang, X. Liu, L. Lai, J. Pei, H. Li, PharmMapper 2017 update: a web server for potential drug target identification with a comprehensive target pharmacophore database. *Nucleic Acids Res.*, 2017, **45**, W356-W360, DOI: 10.1093/nar/gkx374.
23. S. Fang, X. Yu, H. Ding, J. Han, J. Feng, Effects of intracellular iron overload on cell death and identification of potent cell death inhibitors. *Biochem Bioph Res Co.*, 2018, **503**, 297-303, DOI: 10.1016/j.bbrc.2018.06.019.

24. X. Yu, L. Chen, H. Ding, Y. Zhao, J. Feng, Iron Transport from Ferrous Bisglycinate and Ferrous Sulfate in DMT1-Knockout Human Intestinal Caco-2 Cells. *Nutrients.*, 2019, **11**, 485, DOI: 10.3390/nu11030485.
25. Y. Hu, Z. Gui, Y. Zhou, L. Xia, K. Lin, Y. Xu, Quercetin alleviates rat osteoarthritis by inhibiting inflammation and apoptosis of chondrocytes, modulating synovial macrophages polarization to M2 macrophages. *Free Radical Bio Med.*, 2019, **145**, 146-160, DOI: 10.1016/j.freeradbiomed.2019.09.024.
26. R. Rametta, M. Meroni, P. Dongiovanni, From Environment to Genome and Back: A Lesson from HFE Mutations. *Int J Mol Sci.*, 2020, **21**, 3505, DOI: 10.3390/ijms21103505.
27. A. Piperno, S. Pelucchi, R. Mariani, Inherited iron overload disorders. *Translational Gastroenterology And Hepatology*, 2020, **5**, DOI: 10.21037/tgh.2019.11.15.
28. M. W. Hentze, M. U. Muckenthaler, B. Galy, C. Camaschella, Two to Tango: Regulation of Mammalian Iron Metabolism. *Cell*, 2010, **142**, 24-38, DOI: 10.1016/j.cell.2010.06.028.
29. M. Citelli, L. L. Bittencourt, S. V. Da Silva, A. P. Trindade Pierucci, C. Pedrosa, Vitamin A Modulates the Expression of Genes Involved in Iron Bioavailability. *Biol Trace Elem Res.*, 2012, **149**, 64-70, DOI: 10.1007/s12011-012-9397-6.
30. X. Wu, Y. Wang, Q. Wu, W. Cheng, W. Liu, Y. Zhao, C. Mayeur, P. J. Schmidt, P. B. Yu, F. Wang, Y. Xia, HFE interacts with the BMP type I receptor ALK3 to regulate hepcidin expression. *Blood*, 2014, **124**, 1335-1343, DOI: 10.1182/blood-2014-01-552281.
31. H. Kawabata, Transferrin and transferrin receptors update. *Free Radical Bio Med.*, 2019, **133**, 46-54, DOI: 10.1016/j.freeradbiomed.2018.06.037.
32. B. Schaefer, D. Haschka, A. Finkenstedt, B. Petersen, I. Theurl, B. Henninger, A. R. Janecke,

- C. Wang, H. Y. Lin, L. Veits, W. Vogel, G. Weiss, A. Franke, H. Zoller, Impaired hepcidin expression in alpha-1-antitrypsin deficiency associated with iron overload and progressive liver disease. *Hum Mol Genet.*, 2015, **24**, 6254-6263, DOI: 10.1093/hmg/ddv348.
33. L. Silvestri, A. Pagani, A. Nai, I. De Domenico, J. Kaplan, C. Camaschella, The Serine Protease Matriptase-2 (TMPRSS6) Inhibits Hepcidin Activation by Cleaving Membrane Hemojuvelin. *Cell Metab.*, 2008, **8**, 502-511, DOI: 10.1016/j.cmet.2008.09.012.
34. S. J. Dixon, K. M. Lemberg, M. R. Lamprecht, R. Skouta, E. M. Zaitsev, C. E. Gleason, D. N. Patel, A. J. Bauer, A. M. Cantley, W. S. Yang, B. I. Morrison, B. R. Stockwell, Ferroptosis: An Iron-Dependent Form of Nonapoptotic Cell Death. *Cell*, 2012, **149**, 1060-1072, DOI: 10.1016/j.cell.2012.03.042.
35. D. M. Kopustinskiene, V. Jakstas, A. Savickas, J. Bernatoniene, Flavonoids as Anticancer Agents. *Nutrients*, 2020, **12**, DOI: 10.3390/nu12020457.
36. H. van de Waterbeemd, E. Gifford, ADMET in silico modelling: Towards prediction paradise? *Nat Rev Drug Discov.*, 2003, **2**, 192-204, DOI: 10.1038/nrd1032.
37. M. Leopoldini, N. Russo, S. Chiodo, M. Toscano, Iron chelation by the powerful antioxidant flavonoid quercetin. *J Agr Food Chem.*, 2006, **54**, 6343-6351, DOI: 10.1021/jf060986h.
38. M. Guo, C. Perez, Y. Wei, E. Rapoza, G. Su, F. Bou-Abdallah, N. D. Chasteen, Iron-binding properties of plant phenolics and cranberry's bio-effects. *Dalton T.*, 2007, **43**, 4951-4961, DOI: 10.1039/b705136k.
39. A. Raza, X. Xu, L. Xia, C. Xia, J. Tang, Z. Ouyang, Quercetin-Iron Complex: Synthesis, Characterization, Antioxidant, DNA Binding, DNA Cleavage, and Antibacterial Activity Studies. *J Fluoresc.*, 2016, **26**, 2023-2031, DOI: 10.1007/s10895-016-1896-y.

40. A. Cereto-Massague, M. Jose Ojeda, C. Valls, M. Mulero, G. Pujadas, S. Garcia-Vallve, Tools for in silico target fishing. *Methods*, 2015, **71**, 98-103, DOI: 10.1016/j.ymeth.2014.09.006.
41. Y. Ji, B. Li, M. Qiao, J. Li, H. Xu, L. Zhang, X. Zhang, Advances on the in vivo and in vitro glycosylations of flavonoids. *Appl Microbiol Biot.*, 2020, **104**, 6587-6600, DOI: 10.1007/s00253-020-10667-z.
42. O. A. A. Ahmed, A. S. Azhar, M. M. Tarkhan, K. S. Balamash, H. M. El-Bassossy, Antiglycation Activities and Common Mechanisms Mediating Vasculoprotective Effect of Quercetin and Chrysin in Metabolic Syndrome. *Evid-Based Compl Alt.*, 2020, **2020**, 3439624, DOI: 10.1155/2020/3439624.
43. J. Y. Seo, R. P. Pandey, J. Lee, J. K. Sohng, W. Namkung, Y. I. Park, Quercetin 3-O-xyloside ameliorates acute pancreatitis in vitro via the reduction of ER stress and enhancement of apoptosis. *Phytomedicine*, 2019, **55**, 40-49, DOI: 10.1016/j.phymed.2018.07.011.
44. H. Ding, X. Yu, J. Feng, Iron homeostasis disorder in piglet intestine. *Metallomics*, 2020, **12**, 1494-1507, DOI: 10.1039/D0MT00149J.
45. Y. Zhang, D. Wan, X. Zhou, C. Long, X. Wu, L. Li, L. He, P. Huang, S. Chen, B. Tan, Y. Yin, Diurnal variations in iron concentrations and expression of genes involved in iron absorption and metabolism in pigs. *Biochem Bioph Res Co.*, 2017, **490**, 1210-1214, DOI: 10.1016/j.bbrc.2017.06.187.
46. D. Wan, X. Zhou, C. Xie, X. Shu, X. Wu, Y. Yin, Toxicological evaluation of ferrous N-carbamylglycinate chelate: Acute, Sub-acute toxicity and mutagenicity. *Regul Toxicol Pharm.*, 2015, **73**, 644-651, DOI: 10.1016/j.yrtph.2015.09.013.
47. H. Ding, X. Yu, L. Chen, J. Han, Y. Zhao, J. Feng, Tolerable upper intake level of iron

- damages the intestine and alters the intestinal flora in weaned piglets. *Metallomics*, 2020, **12**, 1356-1369, DOI: 10.1039/D0MT00096E.
48. Y. Zhang, Z. Gao, J. Liu, Z. Xu, Protective effects of baicalin and quercetin on an iron-overloaded mouse: comparison of liver, kidney and heart tissues. *Nat Prod Res.*, 2011, **25**, 1150-1160, DOI: 10.1080/14786419.2010.495070.
49. Y. Zhang, H. L. Li, Y. L. Zhao, Z. H. Gao, Dietary supplementation of baicalin and quercetin attenuates iron overload induced mouse liver injury. *Eur J Pharmacol.*, 2006, **535**, 263-269, DOI: 10.1016/j.ejphar.2006.01.067.
50. Y. Li, M. Chen, Y. Xu, X. Yu, T. Xiong, M. Du, J. Sun, L. Liu, Y. Tang, P. Yao, Iron-Mediated Lysosomal Membrane Permeabilization in Ethanol-Induced Hepatic Oxidative Damage and Apoptosis: Protective Effects of Quercetin. *Oxid Med Cell Longev.*, 2016, **2016**, 4147610, DOI: 10.1155/2016/4147610.
51. M. Simunkova, S. H. Alwasel, I. M. Alhazza, K. Jomova, V. Kollar, M. Rusko, M. Valko, Management of oxidative stress and other pathologies in Alzheimer's disease. *Arch Toxicol.*, 2019, **93**, 2491-2513, DOI: 10.1007/s00204-019-02538-y.
52. P. Zhang, L. Chen, Q. Zhao, X. Du, M. Bi, Y. Li, Q. Jiao, H. Jiang, Ferroptosis was more initial in cell death caused by iron overload and its underlying mechanism in Parkinson's disease. *Free Radical Bio Med.*, 2020, **152**, 227-234, DOI: 10.1016/j.freeradbiomed.2020.03.015.
53. Y. Wang, F. Quan, Q. Cao, Y. Lin, C. Yue, R. Bi, X. Cui, H. Yang, Y. Yang, L. Birnbaumer, X. Li, X. Gao, Quercetin alleviates acute kidney injury by inhibiting ferroptosis. *J Adv Res.*, 2021, **28**, 231-243, DOI: 10.1016/j.jare.2020.07.007.

54. X. Li, J. Zeng, Y. Liu, M. Liang, Q. Liu, Z. Li, X. Zhao, D. Chen, Inhibitory Effect and Mechanism of Action of Quercetin and Quercetin Diels-Alder anti-Dimer on Erastin-Induced Ferroptosis in Bone Marrow-Derived Mesenchymal Stem Cells. *Antioxidants*, 2020, **9**, 205, DOI: 10.3390/antiox9030205.
55. J. A. Rothwell, M. Urpi-Sarda, M. Boto-Ordonez, R. Llorach, A. Farran-Codina, D. K. Barupal, V. Neveu, C. Manach, C. Andres-Lacueva, A. Scalbert, Systematic analysis of the polyphenol metabolome using the Phenol-Explorer database. *Mol Nutr Food Res.*, 2016, **60**, 203-211, DOI: 10.1002/mnfr.201500435.
56. M. Leopoldini, N. Russo, S. Chiodo, M. Toscano, Iron chelation by the powerful antioxidant flavonoid quercetin. *J Agr Food Chem.*, 2006, **54**, 6343-6351, DOI: 10.1021/jf060986h.
57. M. Lesjak, R. Hoque, S. Balesaria, V. Skinner, E. S. Debnam, S. K. S. Srari, P. A. Sharp, Quercetin Inhibits Intestinal Iron Absorption and Ferroportin Transporter Expression In Vivo and In Vitro. *Plos One*, 2014, **9**, e102900, DOI: 10.1371/journal.pone.0102900.
58. Y. Tang, Y. Li, H. Yu, C. Gao, L. Liu, S. Chen, M. Xing, L. Liu, P. Yao, Quercetin prevents ethanol-induced iron overload by regulating hepcidin through the BMP6/SMAD4 signaling pathway. *J Nutr Biochem.*, 2014, **25**, 675-682, DOI: 10.1016/j.jnutbio.2014.02.009.
59. X. Zhao, L. Gong, C. Wang, M. Liu, N. Hu, X. Dai, C. Peng, Y. Li, Quercetin mitigates ethanol-induced hepatic steatosis in zebrafish via P2X7R-mediated PI3K/Keap1/Nrf2 signaling pathway. *J Ethnopharmacol.*, 2021, **268**, 113569, DOI: 10.1016/j.jep.2020.113569.
60. H. Jia, Y. Zhang, X. Si, Y. Jin, D. Jiang, Z. Dai, Z. Wu, Quercetin Alleviates Oxidative Damage by Activating Nuclear Factor Erythroid 2-Related Factor 2 Signaling in Porcine Enterocytes. *Nutrients*, 2021, **13**, 375, DOI: 10.3390/nu13020375.

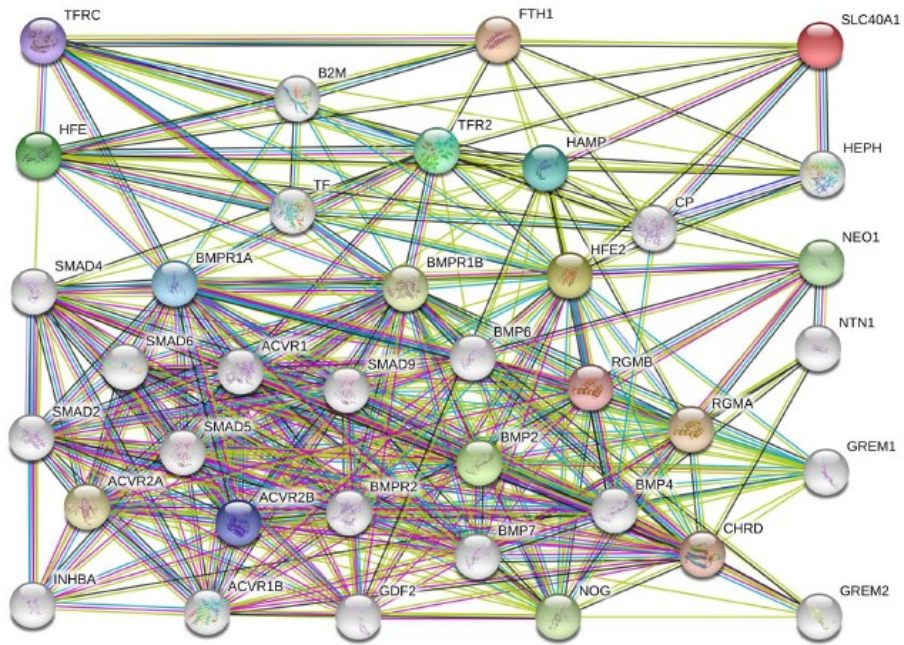


Figure 1. The PPI network of hemochromatosis. Network nodes represent proteins. Edges represent protein -protein associations. colored nodes: query proteins and first shell of interactors. white nodes: second shell of interactors.

ORIGINAL UNEDITED



Figure 2. Gene Ontology (GO) analysis of targets. The Y-axis showed enriched gene ontology categories of the targets, and the X-axis showed the enrichment scores of these terms

ORIC

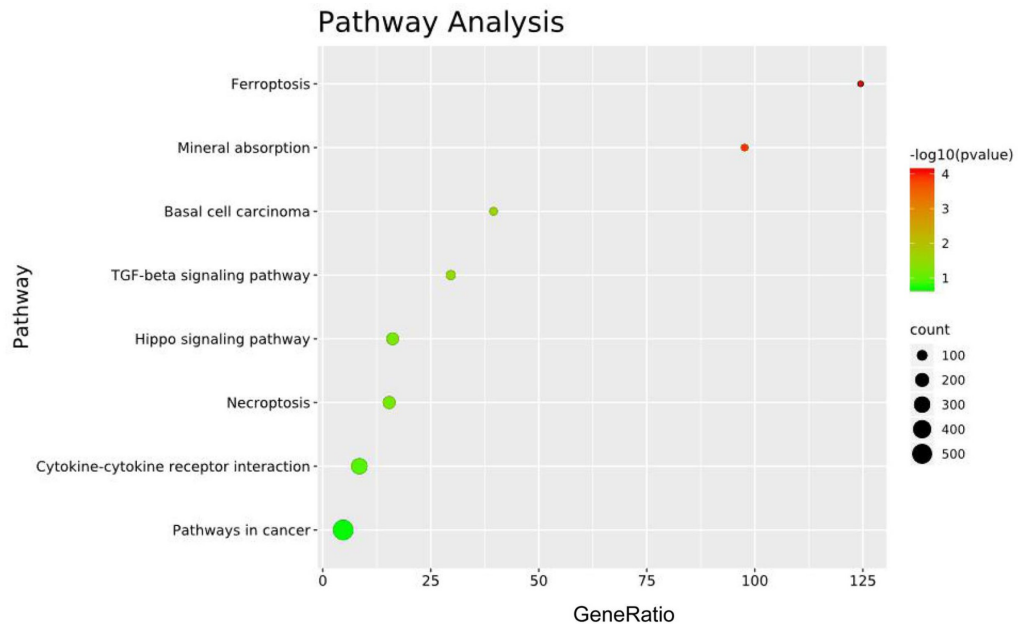


Figure 3. Scatter plot of enriched KEGG pathways statistics. GeneRatio was the ratio of the differentially expressed gene number to the total gene number in a certain pathway. The color and size of the dots represented the range of the $-\log_{10}(pvalue)$ and the number of DEGs mapped to the indicated pathways, respectively. Top 8 enriched pathways were shown in the figure.

ORIGINAL UNEDITED MANUSCRIPT



Figure 4. Gene Ontology (GO) analysis of targets. The Y-axis showed enriched gene ontology categories of the targets, and the X-axis showed the enrichment scores of these terms.

ORIC

ACCEPTED

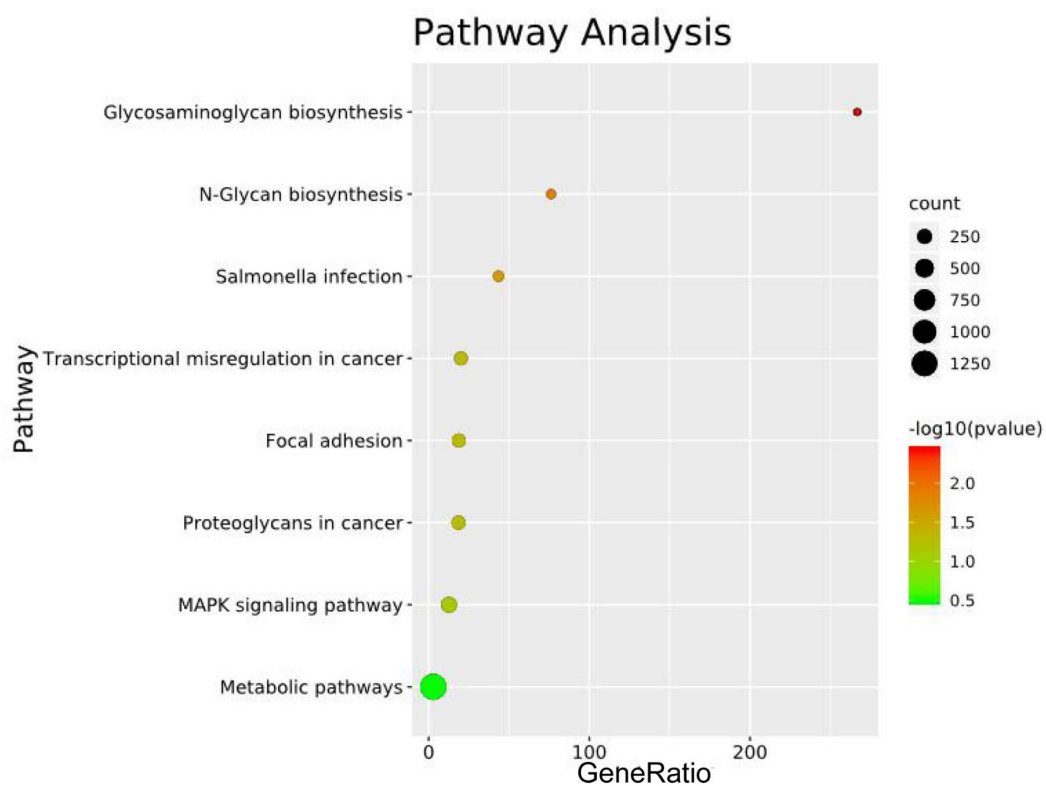


Figure 5. Scatter plot of enriched KEGG pathways statistics. GeneRatio was the ratio of the differentially expressed gene number to the total gene number in a certain pathway. The color and size of the dots represented the range of the $-\log_{10}(pvalue)$ and the number of DEGs mapped to the indicated pathways, respectively. Top 8 enriched pathways were shown in the figure.

ORIGINAL UNEDITED

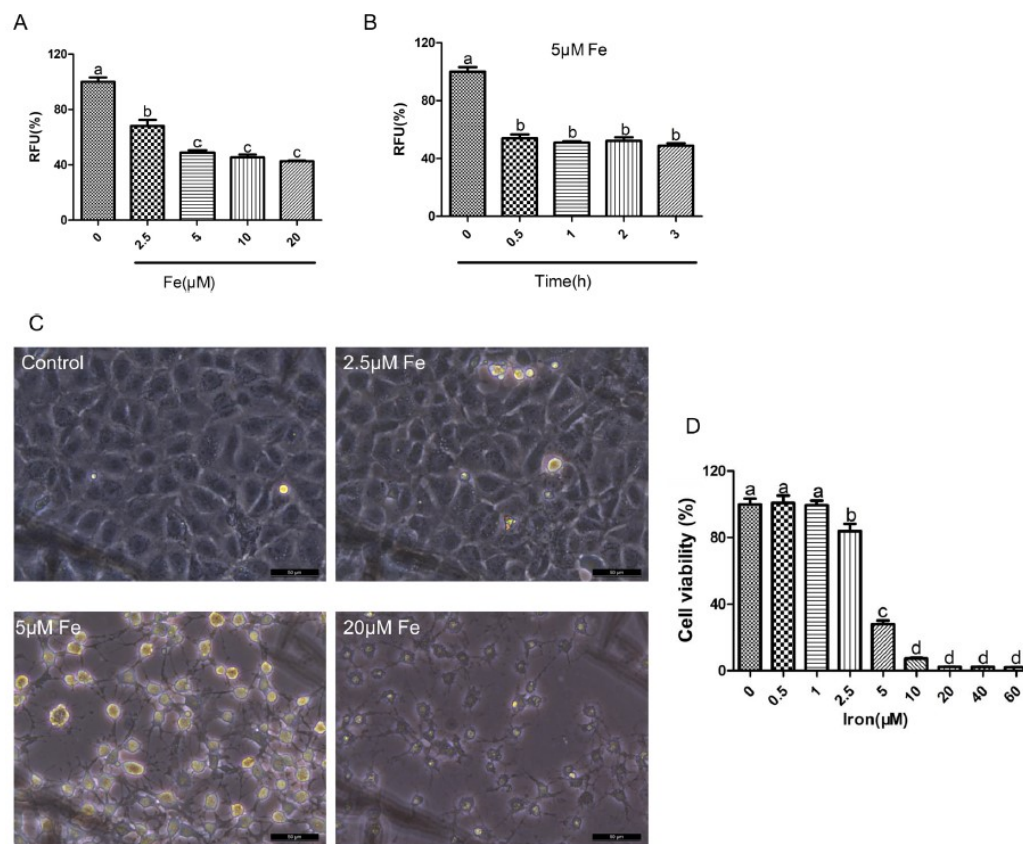


Figure 6. Establishment of iron overload cell model. (A) Changes of intracellular iron after treatment with different iron concentration (0, 2.5, 5, 10, 20 μM) in BRL3A cells. Less Phen Green SK indicated higher concentrations of intracellular iron. (B) Changes of intracellular iron after treated with 5 μM iron for different time (0, 0.5, 1, 2, 3 h) in BRL3A cells. (C) The cell morphology (200x) of BRL3A cells treated with iron (0-60 μM) for 3 hours. (D) The cell viability was evaluated by CCK-8 analysis. Values not sharing a common letter differ significantly ($P < 0.05$).

ORIGINAL

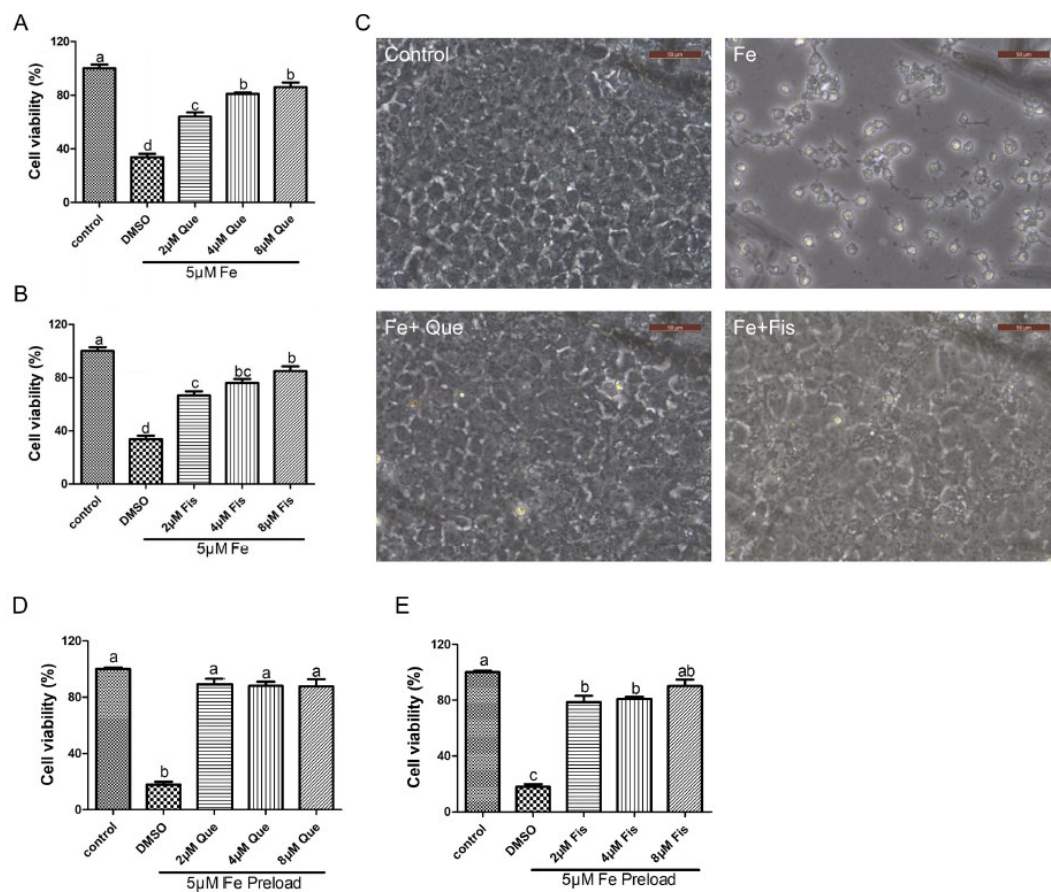


Figure 7. Quercetin protection BRL3A from iron-induced cell death. (A) BRL3A cells were treated with 5 μM iron followed by treatment with quercetin (2, 4 and 8 μM) for 3 h respectively and assessed by a CCK-8 assay. (B) BRL3A cells were treated with 5 μM iron followed by treatment with fisetin (2, 4 and 8 μM) for 3 h respectively and assessed by a CCK-8 assay. (C) BRL3A cells were treated with 5 μM iron followed by treatment with DMSO, quercetin (8 μM) or fisetin (8 μM) for 24 h. The magnification of cell morphology is 200x. (D) BRL3A cells were pretreated with 5 μM iron for 0.5 h, washed with PBS, and then treated with different concentrations of quercetin (0, 2, 4 and 8 μM) for another 2.5h. The cell activity was determined by CCK8 kit. (E) BRL3A cells were pretreated with 5 μM iron for 0.5 h, washed with PBS, and then treated with different concentrations of fisetin (0, 2, 4 and 8 μM) for another 2.5h. The cell activity was determined by CCK8 kit. Values not sharing a common letter differ significantly ($P < 0.05$).

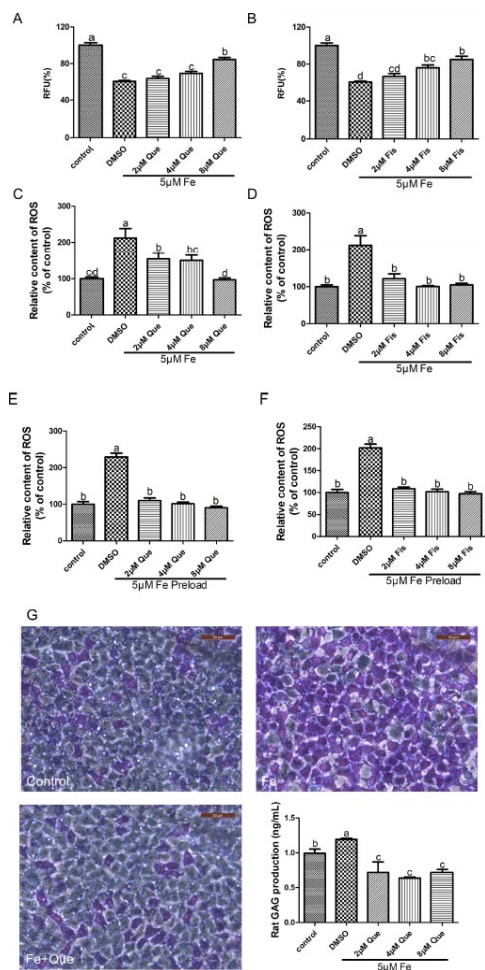


Figure 8. Quercetin-mediated iron, ROS, and GAG clearance. (A) BRL3A cells were treated with 5 μ M iron followed by treatment with quercetin (2, 4 and 8 μ M) for 3 h respectively and assessed by an iron fluorescence. (B) BRL3A cells were treated with 5 μ M iron followed by treatment with fisetin (2, 4 and 8 μ M) for 3 h respectively and assessed by an iron fluorescence. (C) BRL3A cells were treated with 5 μ M iron followed by treatment with quercetin (2, 4 and 8 μ M) for 3 h respectively and assessed by a ROS fluorescence. (D) BRL3A cells were treated with 5 μ M iron followed by treatment with fisetin (2, 4 and 8 μ M) for 3 h respectively and assessed by a ROS fluorescence. (E) BRL3A cells were pretreated with 5 μ M iron for 0.5 h, washed with PBS, and then treated with different concentrations of quercetin (0, 2, 4 and 8 μ M) for another 2.5h. Intracellular ROS level was measured by ROS fluorescence. (F) BRL3A cells were pretreated with 5 μ M iron for 0.5 h, washed with PBS, and then treated with different concentrations of fisetin (0, 2, 4 and 8 μ M) for another 2.5h. Intracellular ROS level was measured by ROS fluorescence. (G) BRL3A cells were treated with 5 μ M iron followed by treatment with quercetin (2, 4 and 8 μ M) for 3 h. Toluidine blue staining was performed to detect the synthesis of glycosaminoglycan. A glycosaminoglycan kit was used to determine the synthesis of glycosaminoglycan in BRL3A. Values not sharing a common letter differ significantly ($P < 0.05$).

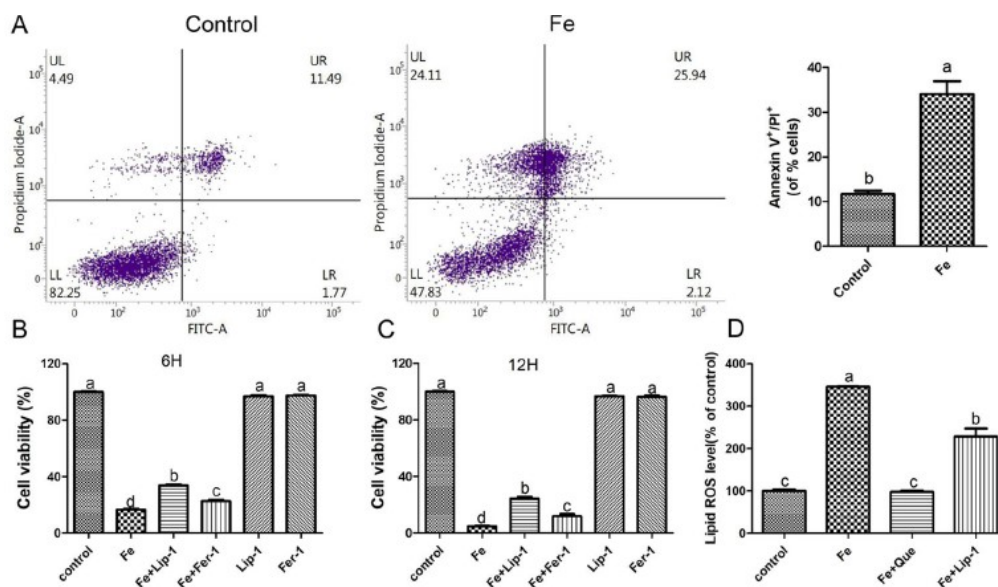


Figure 9. Iron-induced intracellular iron overload causes ferroptosis. (A) BRL3A cells were treated with 5 μ M iron for 3 and detected by flow cytometry. (B) BRL3A cells were treated with 5 μ M iron, 5 μ M iron + 10 μ M Lip-1, 5 μ M iron + 10 μ M Fer-1, 10 μ M Lip-1, 10 μ M Fer-1 for 6 h respectively and the cell viability was measured. (C) RL3A cells were treated with 5 μ M iron, 5 μ M iron + 10 μ M Lip-1, 5 μ M iron + 10 μ M Fer-1, 10 μ M Lip-1, 10 μ M Fer-1 for 12 h respectively and the cell viability was measured. (D) BRL3A cells were treated with 5 μ M iron, 5 μ M iron + 8 μ M Que, 5 μ M iron + 10 μ M Lip-1 for 3 h respectively and lipid ROS level was assayed by flow cytometry using BODIPY 581/591 C11. Values not sharing a common letter differ significantly ($P < 0.05$).

ORIGINAL UNEDITED

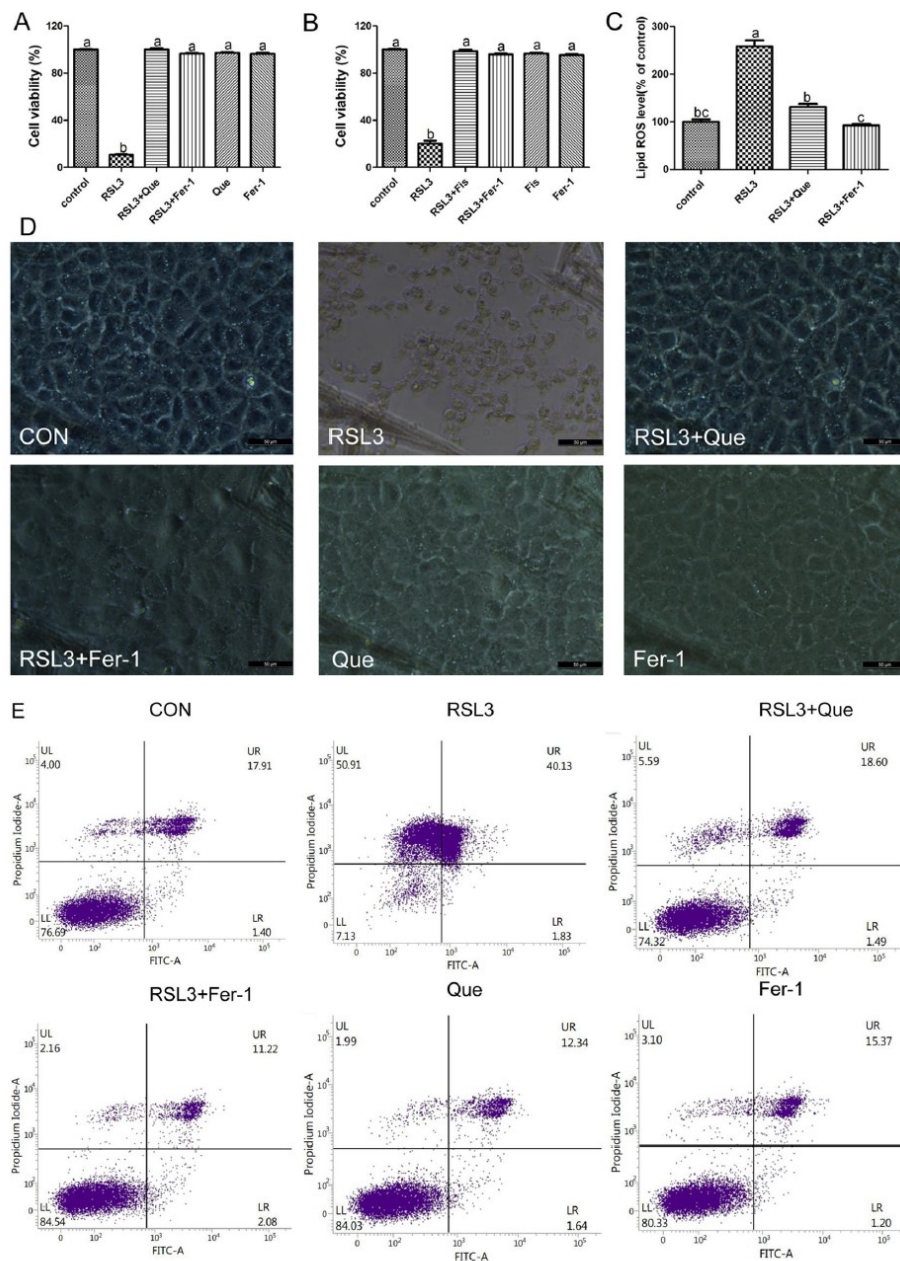


Figure 10. Identification of quercetin as a potent ferroptosis inhibitor. (A) BRL3A cells were treated with 2 μ M RSL3, 2 μ M RSL3 + 8 μ M Que, 2 μ M RSL3 + 10 μ M Fer-1, 8 μ M Que, 10 μ M Fer-1 for 3 h respectively and the cell viability was measured. (B) BRL3A cells were treated with 2 μ M RSL3, 2 μ M RSL3 + 8 μ M Fis, 2 μ M RSL3 + 10 μ M Fer-1, 8 μ M Fis, 10 μ M Fer-1 for 3 h respectively and the cell viability was measured. (C) BRL3A cells were treated with 2 μ M RSL3,

ORIG

RIPT

Table 1. Hemochromatosis target identification from OMIM database.

Number	Location	Gene/Locus	Gene/Locus name	Phenotype
1	1q21.1	HJV, HFE2A	Hemojuvelin	Hemochromatosis, type 2A
2	2q32.2	SLC40A1, SLC11A3, FPN1, IREG1, HFE4	Solute carrier family 40	Hemochromatosis, type 4
3	6p22.2	HFE, HLA-H, HFE1, MVCD7, TFQTL2	Homeostatic iron regulator	Hemochromatosis
4	7q22.1	TFR2, HFE3	Transferrin receptor 2	Hemochromatosis, type 3
5	11q12.3	FTH1, FTHL6, HFE5	Ferritin, heavy polypeptide 1	Hemochromatosis, type 5
6	19q13.12	HAMP, LEAP1, HEPC, HFE2B	Hepcidin antimicrobial peptide	Hemochromatosis, type 2B
7	20p12.3	BMP2, BMP2A, BDA2, SSFSC	Bone morphogenetic protein-2	Hemochromatosis

ORIGINAL UNEDITED MANUSCRIPT

Table 2. Hemochromatosis related compounds were identified from CTD.

Chemical Name	Disease Name	Inference Network	Inference Score
Iron	Hemochromatosis	BMP6 CP HAMP HFE HJV SLC11A2 SLC40A1 TFR2 TNF	36.91
Iron-Dextran Complex	Hemochromatosis	HAMP SLC11A2 TFR2	15.07
Turpentine	Hemochromatosis	HAMP HFE HJV HP SLC11A2 SLC40A1 TFR2 TNF	49.53
ferric ammonium citrate	Hemochromatosis	BMP6 HAMP SLC11A2 SLC40A1 TFR2 TNF	35.35
9-chloro-2-(2-furyl)-(1,2,4)triazolo(1,5-c)quinazolin-5-imine	Hemochromatosis	BMP6 HAMP HJV TFR2	31.05
Deferoxamine	Hemochromatosis	BMP6 CP HAMP SLC11A2 SLC40A1 TFR2 TNF	30.18
gadolinium chloride	Hemochromatosis	BMP2 HAMP HJV SLC40A1 TNF	26.61
Lipopolysaccharides	Hemochromatosis	BMP2 BMP6 CP HAMP HJV HP SLC11A2 SLC40A1 TNF	22.51
Quercetin	Hemochromatosis	AKR1D1 BMP2 BMP6 CP HAMP HP SLC11A2 SLC40A1 TFR2 TNF	22.42
Estradiol	Hemochromatosis	AKR1D1 BMP2 BMP6 CP HAMP HFE HJV HP SLC11A2 SLC40A1 TFR2 TNF	22.27
SU 9516	Hemochromatosis	HAMP HJV TFR2	21.64
kenpallone	Hemochromatosis	BMP6 HAMP TFR2 TNF	21.54
Iron, Dietary	Hemochromatosis	HAMP SLC11A2 SLC40A1 TNF	21.46
cobaltous chloride	Hemochromatosis	AKR1D1 BMP2 BMP6 CP HAMP HFE HP SLC11A2 SLC40A1 TNF	21.00
Cyclosporine	Hemochromatosis	AKR1D1 BMP2 BMP6 CP HAMP HFE HJV HP SLC11A2 SLC40A1 TFR2 TNF	20.63
Ammonium Chloride	Hemochromatosis	AKR1D1 BMP2 BMP6 CP HAMP HFE HP SLC11A2 SLC40A1 TNF	20.14

Table 3. Pharmacological and molecular properties of quercetin.

MW	AlogP	Hdon	Hacc	OB (%)	Caco-2	BBB	DL	FASA-	TPSA	RBN	HL
302.25	1.5	5	7	46.43	0.05	-0.77	0.28	0.38	131.36	1	14.4

Abbreviation: molecular weight (MW); lipid-water partition coefficient (AlogP); hydrogen bond donor (Hdon); hydrogen bond acceptor (Hacc); oral bioavailability (OB); Caco-2 permeability (Caco-2); blood-brain barrier (BBB); drug-likeness (DL); fractional negative accessible surface area (FASA-); topological polar surface area (TPSA); number of rotatable bonds (RBN); half-life (HL)

ORIGINAL UNEDITED MANUSCRIPT

Table 4. Top 30 quercetin similar compounds identification from PubChem database.

number	CID	CMPDNAME	MW	MF	number	CID	CMPDNAME	MW	MF
1	5280343	Quercetin	302.23	C15H10O7	16	5281691	Rhamnetin	316.26	C16H12O7
2	68245	Delphinidin	338.69	C15H11ClO7	17	5281628	Hispidulin	300.26	C16H12O6
3	5280443	Apigenin	270.24	C15H10O5	18	5281605	Baicalein	270.24	C15H10O5
4	439533	Taxifolin	304.25	C15H12O7	19	440735	Eriodictyol	288.25	C15H12O6
5	5281612	Diosmetin	300.26	C16H12O6	20	188323	Cirsimaritin	314.29	C17H14O6
6	5280863	Kaempferol	286.24	C15H10O6	21	5466139	7,8,4'-Trihydroxyiso flavone	270.24	C15H10O5
7	5280445	Luteolin	286.24	C15H10O6	22	5322065	7,3',4'-Trihydroxyfla vone	270.24	C15H10O5
8	72281	Hesperetin	302.28	C16H14O6	23	5320438	Pectolarigenin	314.29	C17H14O6
9	5281672	Myricetin	318.23	C15H10O8	24	5315263	Casticin	374.3	C19H18O8
10	5281670	Morin	302.23	C15H10O7	25	5284649	6,7,4'-Trihydroxyiso flavone	270.24	C15H10O5
11	5281654	Isorhamnetin	316.26	C16H12O7	26	5281894	7-Hydroxyflavone	238.24	C15H10O3
12	5281616	Galangin	270.24	C15H10O5	27	5281666	Kaempferide	300.26	C16H12O6
13	5281614	Fisetin	286.24	C15H10O6	28	5281642	6-Hydroxyluteolin	302.23	C15H10O7
14	5280448	Calycosin	284.26	C16H12O5	29	5281607	Chrysin	254.24	C15H10O4
15	5281701	Tricetin	302.23	C15H10O7	30	5280862	Isokaempferide	300.26	C16H12O6

Table 5. Putative targets of quercetin identified by PharmMapper

Rank	PDB ID	Name	Target Gene	Normalized Fit Score
1	3FER	Filamin-B	FLNB	0.7315
2	2HMA	tRNA-specific 2-thiouridylase	mmA	0.7205
3	2CSX	Methionine--tRNA ligase	metG	0.7182
4	2RFO	Nucleoporin NIC96	NIC96	0.7079
5	2DE0	Alpha-(1,6)-fucosyltransferase	FUT8	0.7054
6	2JZ6	50S ribosomal protein L28	rpmB	0.7049
7	1ZZG	Glucose-6-phosphate isomerase	pgi	0.7014
8	1K7A	Protein C-ets-1	Ets1	0.6828
9	2AEU	UPF0425 pyridoxal phosphate-dependent protein	MJ0158 MJ0158	0.6805
10	2PH7	Uncharacterized protein AF_2093	AF_2093	0.6801
11	1T8E	DNA-directed DNA polymerase	POLQ	0.6774
12	3FFV	Protein syd	syd	0.6749
13	1T9A	Acetolactate synthase catalytic subunit, mitochondrial	ILV2	0.6694